Rydberg atoms in far-infrared radiation fields. II. Wave packet dynamics

J. H. Hoogenraad,* R. B. Vrijen, and L. D. Noordam[†]

FOM Institute for Atomic and Molecular Physics, Kruislaan 407, 1098 SJ Amsterdam, The Netherlands

(Received 30 July 1997)

The short-pulse dynamics of excitation and stimulated emission between highly excited states ($15 < n < 60$) is studied with picosecond far-infrared pulses (40–60 μm) originating from a free electron laser. We measured the excitation of a Rydberg wave packet in rubidium around $n=40$ excited from a deeper bound ($n \approx 20$) Rydberg state by a picosecond far-infrared laser pulse. Moreover, starting from a stationary $n=40$ state we found that upon irradiating with a short far-infrared laser pulse, adjacent Rydberg states are populated by resonant Raman transfer via a deeper ($n=20$) bound state. Finally, we discuss the dynamics of wave-packet excitation at a Cooper minimum in lithium, where sign change of the excitation matrix elements causes excitation at large distances from the atomic core. Possible measurement methods for this effect are discussed and found to yield different information. [S1050-2947(98)09205-1]

PACS number(s): 32.80.Rm, 32.80.Qk, 41.60.Cr

I. INTRODUCTION

In this second paper of the series entitled ''Rydberg atoms in far-infrared radiation fields'' we present short-pulse effects in Rydberg atoms, induced by picosecond far-infrared (FIR) radiation. We have used radiation from the free-electron laser for infrared experiments (FELIX) as a source of FIR radiation for the Rydberg atom experiments. We use its wide, controllable bandwidth ($\Delta\lambda/\lambda = 0.2 - 10\,\%$) to excite either a single state or a superposition of neighboring states (a Rydberg wave packet) [1,2]. The large bandwidth implies short enough pulses to excite wave packets in the high-lying Rydberg states. Recently, wave packets have been widely studied using laser pulses of visible wavelengths [3–5]. Here, we discuss differences in the excitation of Rydberg wave packets by far-infrared radiation starting from another Rydberg state, and compare this to excitation by optical radiation from the ground state.

In Sec. II we summarize some of the results obtained with laser pulses in the visible region. These results can be interpreted in terms of the classical analog of a Rydberg state, an electron on a Kepler orbit. Upon exciting a wave packet, an electron is launched on its orbit from the core region. Section III generalizes these notions. We show that for the excitation of a wave packet with far-infrared radiation, the radial region that contributes to the excitation is larger than for visible excitation. We also show that the *fraction* of the lower-lying state that contributes to the photoexcitation is small. Section IV presents measured wave-packet population in rubidium. Starting from an $n \approx 20$ state, we show the excitation of a wave packet with pulses of only a few optical cycles of a FIR field at 218 cm^{-1} (cycle time 150 fs). At the same wavelength, we observed redistribution of population, starting from a stationary $n \approx 40$ state, to neighboring states. Section V shows that this process is efficient if a lower-lying state is resonant within the bandwidth of the short pulse. In Sec. VI

we present calculations on the excitation of a wave packet near a bound-bound Cooper minimum in lithium. This wave packet has no classical analog. Instead, two wave packets are created that interfere destructively at the classical orbit position, near the core. For the calculations in this paper, we use the calculated elements [6] for the Rydberg-Rydberg transitions.

II. RYDBERG WAVE PACKETS

The classical analog of a Rydberg state is an electron on a Kepler orbit. In this picture, the electron orbits the core of the atom like a planet orbits the sun. A classical particle can be described as a wave packet, or superposition of quantum-mechanical states [1,2]. As the eigenenergies of these states differ slightly, the orbit time is reflected in ''quantum beats'' in the observables. The orbit time is several picoseconds for the Rydberg states we have studied. Radial wave packets are formed [7] upon exciting Rydberg states with picosecond optical pulses, that have a pulse duration shorter than this orbit time. Hence, the bandwidth of such pulses is larger than the Rydberg energy spacing, and the excited Rydberg wave packet is a nonstationary superposition of Rydberg states. The wave function $\psi(r,t)$ after excitation of a wave packet with a short pulse is given by

$$\psi(r,t) = \sum_n a(n) e^{i\omega_n t} \psi_n(r) \equiv \sum_n b(n,t) \psi_n(r), \quad (1)$$

$$a(n) = F(\omega_n - \omega_{\text{init}}) \langle \psi_n | r | \psi_{\text{initial}} \rangle, \quad (2)$$

where $\psi_n(r)$ are the eigenfunctions, ω_n the eigenenergies, and a_n the initial amplitudes of the contributing Rydberg states. The amplitudes of the states are determined by the amplitude spectrum $F(\omega)$ of the excitation pulse and the excitation matrix elements $\langle \psi_n | r | \psi_{\text{initial}} \rangle$ for exciting state n. Under most circumstances, the matrix elements are constant up to a scaling factor that normalizes the excited population to the density of states. Immediately after exciting with a Gaussian pulse, a wave packet is excited which is optimally

---

  *Present address: Philips Research Laboratories, Box WB-21, Prof. Holstlaan 4, NL-5656 AA Eindhoven, The Netherlands.

  [†]Author to whom correspondence should be addressed.

confined at the core, since photoexcitation from the ground state takes place near the core.

After excitation, the wave packet moves out to the outer turning point of its orbit, and returns after one round-trip time. This round-trip time is the inverse of the level spacing of the states that make up the wave packet. The spacing of the states is not equal for all neighboring-state pairs. Due to this anharmonicity, the wave packet disperses. After a few round-trip times, the wave packet has broadened beyond recognition. On a longer time scale, the same dispersion causes the wave packet to be recreated in so-called revivals [8]. These phenomena have been studied, and are parametrized by the spacing of the states, and its variation [9].

III. SHORT-PULSE PHOTOABSORPTION IN THE FAR-INFRARED REGION

In this section we discuss the differences in a Rydberg wave packet excited either by a short laser pulse starting from the ground state (optical excitation) or by starting from a stationary Rydberg state (FIR excitation). Starting from the ground state, the size of the lowest-state wave function limits the area in which population can be transferred to the Rydberg states to a_0. The excited Rydberg wave packet is therefore initially confined. In the far-infrared region, however, the overlap between two Rydberg states extends much further, and one expects that much larger areas of the wave function contribute to the population transfer. We estimate the effective radius contributing to the population transfer by inspecting the matrix elements. Assuming that $\Delta n \ll n$ the semiclassical FIR matrix elements reduce to [6]

$$\langle n + \Delta n | r | n \rangle \approx C n^2 (\Delta n)^{-5/3}. \tag{3}$$

For $\Delta n = 0$, the expectation value of r is known: $\langle n | r | n \rangle \approx n^2$. This is the size of the Rydberg wave function. If $\Delta n \neq 0$, the wave functions of the two states will deviate most in the remote region. The net contribution to $\langle n + \Delta n | r | n \rangle$ from this remote region is very small. Near the core, the Coulomb potential is much stronger than the binding energy of the electron, and the wave function will be little affected by a change in Δn. Therefore Eq. (3) can be used to approximate the fraction of the wave function (near the core) that contributes to the matrix elements. After normalizing to n^2 to remove the total size of the wave function, we find that this is a fraction $(\Delta n)^{-5/3}$ of the wave function. For example, if we excite an $n = 30$ state to states near $n = 40$, the inner 2% $(20a_0)$ of the initial wave function contributes to the population transfer. In summary, FIR Rydberg transitions still take place in a restricted area near the core. However, the size of that area (tens of a_0) is substantially larger than for excitation from the ground state (a_0).

The modified excitation can also be described in terms of the laser bandwidth exciting a Rydberg wave packet. Upon deriving the shape of the wave packet, the optical excitation matrix elements were assumed to be independent of the wavelength, apart from a density of states effect [2]. The relative bandwidth $(\Delta \omega / \omega)$ required to excite more than one Rydberg state in the far infrared is enormous by optical standards: 5%. From semiclassical approximations, we found that the amount of excited population acquires an additional scaling factor of $\omega^{-10/3}$ [6]. Due to the large far-infrared bandwidth, the cross sections for far-infrared excitation are no longer constant within the bandwidth of the pulses. The matrix elements increase rapidly with decreasing transition frequency. Therefore a wave packet is excited with frequency components centered around a lower n than expected from the central frequency of the radiation field. The different contributing states cause the initial wave packet, with an envelope of the population distribution that is no longer a Gaussian, to spread out beyond the core region. Starting from a Rydberg state instead of starting from the ground state, the wave-packet excitation is thus no longer restricted to the core region.

IV. WAVE PACKET POPULATION MEASUREMENTS

We have measured the excited wave packet after exposing rubidium Rydberg states to picosecond FIR pulses. We refer to Ref. [10] for a more extensive description of the experimental setup, which resembles the one from Ref. [11]: In a vacuum system ground-state rubidium atoms, coming from a resistively heated oven, are two-photon excited to an initial nd state. Directly after excitation the Rydberg atoms are exposed to radiation from the FELIX free-electron laser [12]. Every 200 ms, FELIX generates a macropulse, consisting of a train of about 5000 micropulses. The short (picosecond) micropulses in the macropulse are repeated at 1 GHz (1 ns interval time). These pulses are incoherent on the time scale that the atoms experience. By firing the dye laser during the macropulse, we select approximately 850 pulses. The frequency of FELIX can be scanned continuously from 5 to 110 μm. The bandwidth (and thus the pulse duration of the micropulses) can be varied independently of the continuously tunable frequency. In our vacuum system, the FIR beam is focused by a parabolic mirror to a <1 mm spot. By adjusting the timing of the dye lasers with respect to the FIR laser, the number of micropulses to which the Rydberg atoms are exposed can be selected. The electrons released in the multiphoton ionization process are pushed to a multichannel plate detector by a static field of 5 V/cm. After every FIR pulse train, a slowly ramped electric field ionizes Rydberg states above the initial-state. Since different Rydberg states ionize at different field strengths of the ramped electric pulse, the time of arrival of the electrons at the detector is mapped to binding energies. The dye lasers operated on twice the repetition frequency of the FIR laser, yielding a reference shot for each FIR shot. We will show the signal from these shots as an initial-state signal.

In the experiment, either the Rb $20d$ or $21d$ state was excited with 218 cm^{-1} FIR radiation to a wave packet around $n = 40$, using two different relative bandwidths: 1.5% and 5%. These bandwidths correspond to 30 and nine cycles per FIR pulse, or 4.5 and 1.4 ps. These pulses are shorter than the round-trip time of 10 ps of a Rydberg electron around $n = 40$, but longer than the round-trip time of 2 ps of a Rydberg electron around $n = 20$. Figure 1 shows the population redistributions after the FIR pulse train [10]. The leftmost peak of each spectrum shows remaining initial-state population. With a dotted line, we have shown the signal without FIR radiation. To the right, one finds the population distribution over the $n \approx 40$ states after the FIR radiation. The
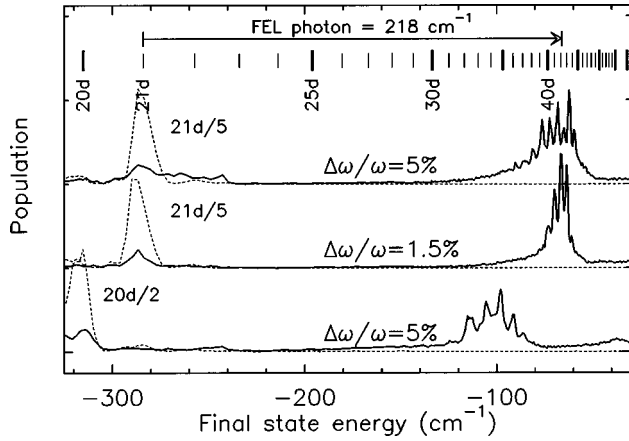
FIG. 1. Rydberg-state distributions as probed with state-selective field ionization after excitation of the rubidium 20d and 21d states to higher-lying states using 218 cm^{-1} FIR radiation. Trace (a): 21d and 1.5% bandwidth FIR (4.5 ps, 30 cycles). Trace (b): 21d and 5% bandwidth FIR (1.4 ps, nine cycles), and trace (c): 20d and 5% bandwidth FIR (1.4 ps, nine cycles). The atoms were submitted to approximately 850 ns of radiation. In trace (a) the average intensity was 20 kW/cm^2. Of the population, 10% remained in the initial state, 60% was excited to the high-Rydberg states, and 5% was ionized. For traces (b) and (c) (5% bandwidth) the average intensity was 30 kW/cm^2. In trace (b), 5% of the population remained in the initial state, 90% was excited to the high-Rydberg states, and 5% was ionized, while for trace (c) these numbers were 10%, 80%, and 10%, respectively. The dotted lines show spectra of the initial state as obtained from reference shots without FIR radiation. The heights of the spectra are scaled with the factors shown near the peak.

two-photon ionization signal of a few percent of the population is not shown. Figure 1 demonstrates that the number of populated Rydberg states depends on the applied bandwidth [compare trace (a) with $\Delta\lambda/\lambda = 5\%$ and (b) with $\Delta\lambda/\lambda = 1.5\%$], while the central n populated is defined by the photon energy and the initial state [compare traces (b) and (c)].

V. ANTI-WAVE-PACKETS: NEIGHBORING-STATE POPULATION

So far, the orbit time of the initial state was much shorter than the pulse duration. In this section, we *start* in a higher-lying state, with an orbit time longer than the pulse duration. From the dynamics of the deexcitation follows that neighboring states near the initial state are excited. Again the argument holds that the excitation takes place near the core: Only the part of the wave function of a high-lying, initial, state that is near the core interacts with electromagnetic radiation during a short laser pulse. The laser pulse drills a hole, or anti-wave-packet, into the wave function. For pulses shorter than the Kepler orbit time ($\tau_p < \tau_n$), only a small fraction of the wave function nears the core, and it is shown that complete ionization is prohibited [13,14]. This is quantum mechanically described as populating neighboring Rydberg states by Raman transfer via continuum states [15,16]. Using optical pulses, Raman transfer via a low-lying state has been demonstrated [17,18]: The atom is first deexcited to a lower-lying state, followed by the coherent excitation of a wave
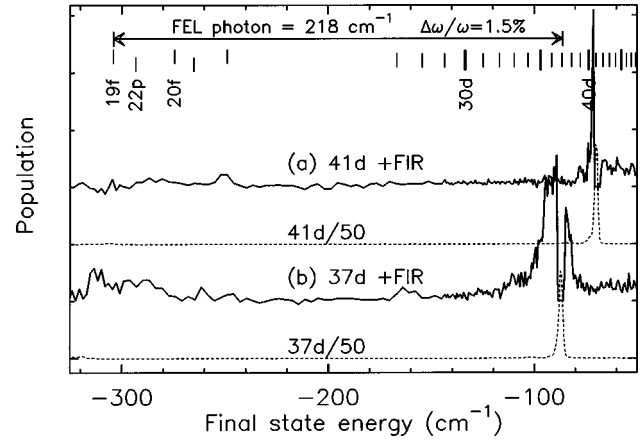

FIG. 2. Redistribution to neighboring states using approximately 850 ns of radiation with an average intensity of 20 kW/cm^2 at 218 cm^{-1} with 1.5% bandwidth (4.5 ps, 30 cycles). The full lines show the Rydberg population, with the remaining initial-state population subtracted. Trace (a) shows the population distribution after irradiating the 41d state, with 0.32 times the initial-state distribution subtracted and trace (b) after irradiating the 37d state with 0.14 times the initial-state distribution subtracted. The dotted lines show the initial-state population in absence of FIR radiation.

packet in states neighboring the initial state. This coherent superposition may then be hardly ionizable, just like the dynamical stabilization that is found in microwave ionization [19–21].

We have studied this neighboring-state redistribution via a deeper-bound state at the same FIR frequency as the wave-packet excitation in Sec. IV. Figure 2(b) shows the neighboring-state population after exposing the 37d state to 218 cm^{-1} FIR radiation with 1.5% bandwidth. The 37d-19f resonance lies within this bandwidth. The remaining total high-Rydberg population is 40% of the original amount. For the overlap of the initial and final spectra, we have determined that 15% remained in the initial state. Figure 2(b) shows the field-ionization spectrum, with this fraction of 15% of the initial-state spectrum subtracted. The neighboring states have 25% of the original population. This is more than remains in the initial state. On the left, the population of the 19f state (about 5%) is shown. We observed about 5% ionization. We can now compare the 37d redistribution with what happens when we irradiate the 41d state with the same radiation [Fig. 2(a)]. Since at this wavelength, the laser is detuned from the 41d-20f resonance, while the much weaker [10,6] high-d to low-p transition (41d-22p at 223 cm^{-1}) also lies outside the bandwidth of the pulse, one observes that little redistribution takes place starting from the 41d state. Of the 45% population remaining in the high-Rydberg states, 32% remains in the initial state, and only 13% is redistributed. The low-Rydberg state is negligible, and again about 5% is ionized. In both cases about half of the population disappears from the spectra, and is most likely transferred to deeper-bound states (see also Ref. [10]).

Figure 3(a) shows the results of an experiment similar to Fig. 2 after we have increased the bandwidth of the FIR radiation to 5%. As expected, the final-state distribution after irradiating the 37d state broadens. After the pulse train, the high-Rydberg population is much larger than the population
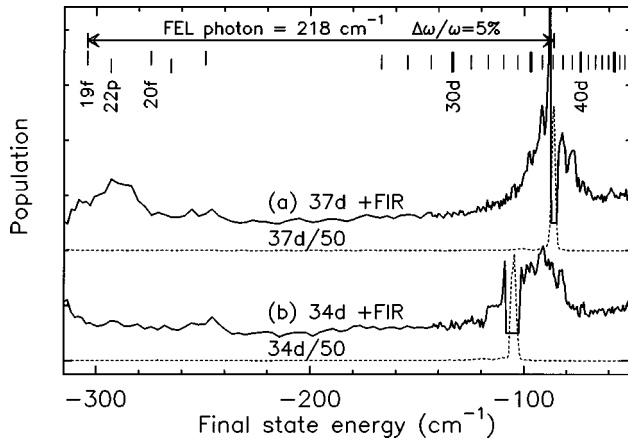
FIG. 3. Redistribution to neighboring states using approximately 850 ns of radiation with an average intensity of 40 kW/cm^2 at 218 cm^{-1} with 5% bandwidth (1.4 ps, nine cycles), plotted like Fig. 2. Trace (a) shows redistribution from the 37d state (0.13 times initial state subtracted) and trace (b) redistribution from the 34d state (0.21 times initial state subtracted).

in the 19f, even though population redistribution uses the 19f state as an intermediate state. Of the population, 37% remains in the high-Rydberg states, of which 13% is in the initial state, and 24 % in neighboring states. Finally, Fig. 3(b) shows the population distribution after exposing the 34d state to the larger-bandwidth pulse. This redistribution is again dominated by transfer via the 19f state. The asymmetric population redistribution is centered around the 37d state (rather than the initial 34d state), indicating the strong resonant effect. The intermediate state, however, lies barely within the bandwidth, so that populating the 19f is less efficient. This is confirmed by the observation that 44% of the population remains in the high-Rydberg states, of which 21% is in the initial state, and 23% in neighboring states. About 8% is ionized in a two-photon process. The transfer away from the 34d is indeed less efficient than transfer from the 37d state.

Let us now consider what would happen if the bandwidth were further increased, and thus the pulses were further shortened. In that case, several *lower-lying* states lie within the bandwidth, and a wave packet of the lower-lying states is excited. This excitation takes place over a finite range near the core (see Sec. III). The hole, or anti-wave-packet in the initial, high-lying wave function is deexcited to a localized wave packet in the final, lower-lying state. Both the wave packet and the anti-wave-packet move out on their own orbits after the pulse. The radial parts of both wave packets will move out with approximately the same velocities [see, e.g., Eq. (6) of Ref. [6]]. Only when the outer turning point of the inner orbit is approached do the wave packets part. The angular distributions of the deexcited wave function and of the initial-state wave function are not the same. Pump-probe techniques can be used to follow the dynamics of both wave packets, and to see the inner wave packet return to the core first. Of course, similar dynamics govern the excitation of high-lying Rydberg states from a lower-lying initial state. Initially, the excited wave packet moves along with the anti-wave-packet of the initial state, until the anti-wave-packet reaches its outer turning point.

VI. COOPER-MINIMUM WAVE PACKETS

In Sec. III we have noticed that the excited wave packet changes as the excitation matrix elements of the individual states in the wave packet change. This effect is dramatic for excitation near a minimum in the cross section, where even the sign of the matrix elements changes. Such a minimum occurs for the far-infrared $s \rightarrow p$ Rydberg transitions in lithium [10,6,11]. Here, we present calculations on a wave packet excited at a Cooper minimum. The interference between states that is required for the formation of a wave packet is severely changed due to the sign change that accompanies the minimum.

If the matrix elements in Eq. (2) are approximately constant, it is shown that a wave packet, excited with a short pulse, fills a fraction of the Kepler orbit given by the ratio of the pulse duration and the Kepler orbit time τ_n. The wave packet is excited near the core and moves out during the laser pulse. The wave-packet spectrum created by a Gaussian pulse, centered around ω_0, is

$$a(n) = C e^{-[(\omega_n - \omega_0)/(0.5\Gamma)]^2}, \quad (4)$$

with Γ the power bandwidth of the pulse and C the approximately constant common matrix elements. If the central frequency coincides with a Cooper minimum, the excitation matrix elements scale linearly with the detuning. The effective excitation spectrum of a Gaussian pulse changes therefore to

$$a_{\text{Cooper}}(n) = (\omega_n - \omega_0) C' e^{-[(\omega_n - \omega_0)/(0.5\Gamma)]^2}, \quad (5)$$

with C' a prefactor of the matrix elements.

The amplitudes of the Rydberg states $[a(n)]$ are given by the *effective* pulse shape: the product of the *real* optical pulse shape and the matrix elements. We will first discuss the shape of a wave packet excited near a Cooper minimum in terms of this effective pulse shape, while keeping hydrogenic matrix elements. We can then use the classical correspondence for the excited wave packet, and use the knowledge of the temporal pulse shape of Eq. (5), to infer the shape of a wave packet excited near a Cooper minimum.

The temporal pulse shape of bandwidth-limited pulses can be determined by squaring its Fourier-transformed frequency spectrum. For both excitation spectra [Eqs. (4) and (5)] it is observed that they have the same pulse shape in the frequency and time domain. In both cases, the pulse shape resembles the effective *power* spectrum [the square of Eqs. (4) and (5)]. A bandwidth-limited pulse with a Gaussian frequency spectrum [Eq. (4)] is again Gaussian, and narrows as the frequency spectrum widens. Likewise, the pulse shape resulting from Eq. (5) is doubly peaked, like its power spectrum. The time between the two peaks is equal to the original excitation pulse length: $2\pi/\Gamma$ [easily verified by differentiating Eq. (5)].

The single, Gaussian pulse [Eq. (4)] excites a single well-localized wave packet. The doubly peaked *effective* pulse [Eq. (5)] excites wave packets at both the rising and the falling edge of the *real* pulse. Meanwhile, the excited population moves out radially, so that the excited wave packet spatially resembles the effective temporal pulse shape.
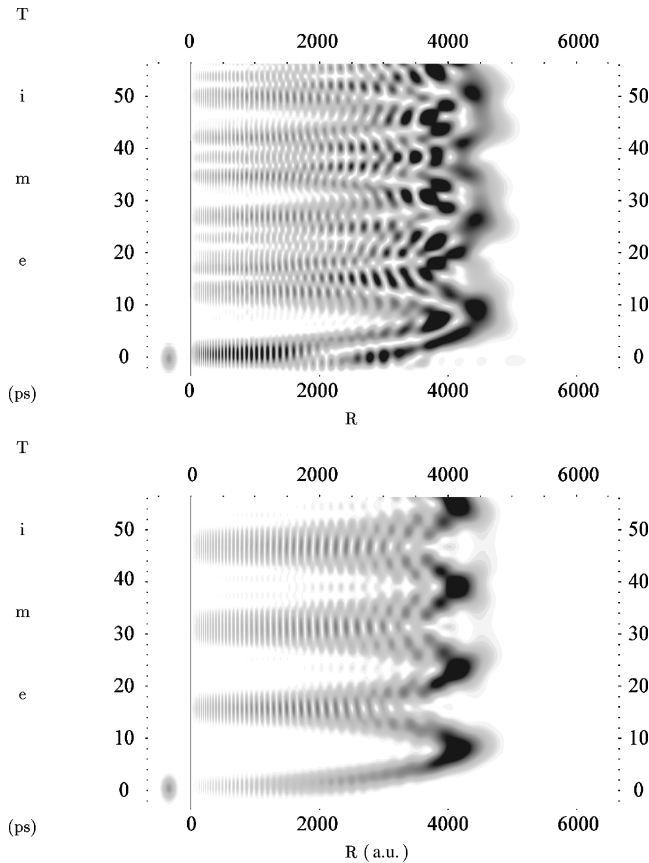
FIG. 4. The evolution of the radial wave function $r^2|\psi(r)|^2$ after exciting a wave packet around the $46p$ state in lithium excited with a 3 ps FIR pulse from (a) the $22s$ state and (b) the $22d$ state. The (hydrogenlike) wave packet excited from the $22d$ state starts at the core, and returns as a whole after each round-trip time of 15 ps. The wave packet excited through the $22s$-np Cooper minimum, however, is broken into two parts. At an integer times the round-trip time, no wave function is present at the core. The excited-state distributions for both curves are shown in the inset of Fig. 5. To the left of the wave packet, the light intensity is shown as gray intensity on the same time axis.

Figure 4(b) shows a calculated wave packet excited in the p series around the Li $46p$ state from a d-state, with normal, hydrogenic matrix elements. From the $22d$ state, f states could also be excited, giving similar radial behavior of the wave packet. For the $22s$ state in Fig. 4(a), the center of the frequency spectrum coincides with a Cooper minimum, so that Eq. (5) applies. The doubly peaked structure is clearly visible at 7 ps at the outer turning point. The return to the core, at 15 ps, also occurs in two parts.

Note that the wave-packet shape *during* the excitation does not have the doubly peaked structure. The description given above, with a fixed *effective* pulse shape, is only valid *after* the pulse: During the pulse, the atom has only experienced a fraction of the pulse. The bandwidth of that part of the pulse is larger and far-detuned states still contribute to the wave packet at early times. These detuned states contribute symmetrically, but with opposite sign: the wave packet starts far from the core. Near the core, all contributing Rydberg states interfere destructively. During the pulse, this remote wave packet moves towards the core, where a standing wave pattern builds up. The phase of this standing wave is
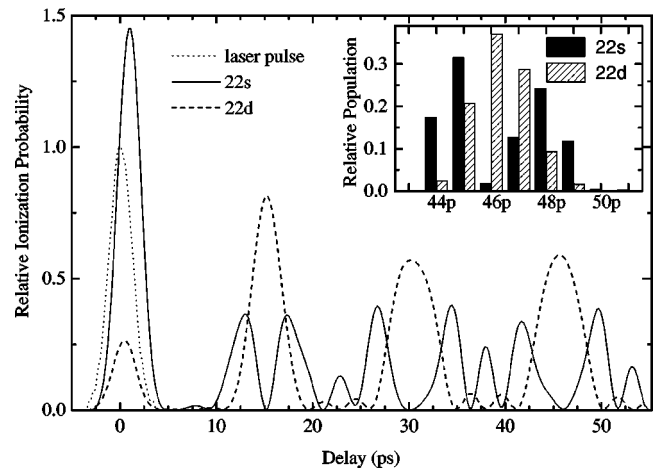

FIG. 5. Relative ionization probabilities $|\Sigma_n b(n,t)|^2/$ $[\Sigma_n|b(n,\infty)|]^2$ as a function of the time t between the excitation and the ionization pulse for the $46p$ state ($\tau_n=15$ ps) in lithium excited from the $22s$ state with a 3 ps pulse at 184 cm^{-1}. A calculation for excitation from the $22d$ state, at a lower intensity to normalize the average excitation probability, is shown with the dashed line. The dotted line shows the excitation pulse. The excited-state distributions $|b(n,\infty)|^2/\Sigma_n[|b(n,\infty)|^2]$ for both curves are shown in the inset.

such that the population from the far-detuned states is pumped back to the initial state. Only population in states within the bandwidth given by Eq. (5) remains after the pulse. Interestingly, the total population in the Rydberg states decreases as a function of the pulse duration for pulses of a constant intensity. For a normal, hydrogenic system, the population in the Rydberg states increases under these circumstances, as the fluence of the pulses increases.

The wave packet can be probed by photoionization, or by any other process that is sensitive to $|\Sigma b(n,t)|^2$ [cf Eq. (1)]. This quantity is displayed in Fig. 5 for the wave packets shown in Fig. 4, normalized to the total excited amplitude. The hydrogenlike wave packet excited from the $22d$ state starts at the core during the pulse. After one round-trip time (at 15 ps), the wave packet returns to the core. At this return, a standing wave builds up from the incoming and outgoing wave packet, increasing the peak height by a factor of 4 with respect to the peak at $t=0$. The wave packet broadens in successive returns due to dispersion.

For excitation from the $22s$, a Cooper-minimum wave packet is created and the returns show a *doubly* peaked structure. The split recurrence near the $22d$ recurrence corresponds to two wave packets that are excited by the two peaks in the effective time profile of the laser pulse. In the middle, at the point where the wave packet is classically expected, the two parts of the wave packet interfere destructively. Note that during the excitation of the wave packet, *more* population is excited than after the pulse. The ionization probability, normalized to the maximal probability *after* the pulse, therefore exceeds 1.0 during the excitation of the wave packet.

Rydberg wave packets can be probed by ionization with a time-delayed second pulse. The ionization matrix elements from the Li p states are nearly hydrogenic for ionization to both the s and the d continuum [6]. These matrix elements vary little as a function of the initial state. The photoioniza-
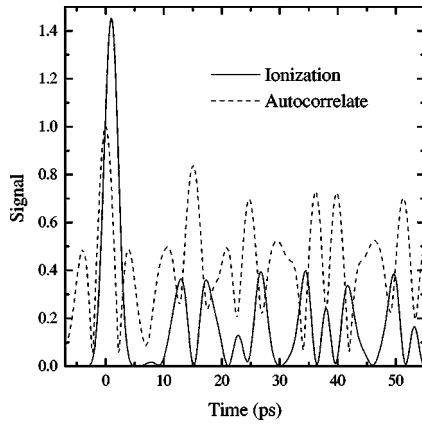
FIG. 6. Relative ionization probabilities $|\Sigma_n b(n,t)|^2/[\Sigma_n|b(n,\infty)|]^2$ as a function of the time t between the excitation and the ionization pulse (as in Fig. 5) compared to the magnitude of the autocorrelation function $|\langle\psi(0)|\psi(t)\rangle|=|\Sigma_n|b(n,\infty)|^2 e^{i\omega_n t}|/\Sigma_n[|b(n,\infty)|^2]$ as a function of the delay time t.

tion signal probed by a second pulse therefore exhibits the time behavior as depicted in Fig. 5.

Finally, we remark that using the Ramsey interference technique [22–24] to probe the wave packet, instead of photoionization, would result in a completely different observation, as shown in Fig. 6. In the Ramsey interference technique, a delayed probe pulse is used for either stimulated emission to or additional excitation from the initial state. This technique measures the (auto) correlate of a wave packet that has evolved in time and a just excited wave packet [25]. Because the second excited wave packet *also* experiences the Cooper minimum, the reference wave packet is *not* localized at the core. The destructive interference at integer round-trip times is therefore not visible. Ramsey *autocorrelates* are not sensitive to the *phase* of the excited wave packet [24]. Probing with Ramsey autocorrelates discards the sign change from Eq. (5). The autocorrelate shows the double peaks of the effective excitation spectrum at -3 ps and $+3$ ps. This pattern repeats at every round-trip time, and disperses in the mean time, giving rise to the complicated structures shown in Fig. 6.

Note that the Fourier transform of the power spectrum $[I(\omega)=|F(\omega)|^2]$ corresponding to Eq. (5) does not give the same result as squaring the Fourier transform of the amplitude spectrum. The pulse shape of Eq. (5) is thus *not* equal to the Fourier transform of its power spectrum as this Fourier transform neglects the sign change in Eq. (5). Analogously to the Fourier transform of the power spectrum of a pulse shaped like Eq. (5) not representing its pulse shape, the Ramsey autocorrelate does not probe the wave packet's shape.

VII. SUMMARY

Using far-infrared picosecond pulses from a free-electron laser, we have investigated atomic Rydberg wave packets. The excitation probabilities show a dependence on the frequency within the large bandwidth of the picosecond far-infrared pulses. We have excited these wave packets in rubidium. Even more, we have created holes in the wave function by irradiating a single, highly excited Rydberg state with radiation that is shorter than the electron round-trip time. Population is redistributed from the single initial Rydberg to several neighboring states. Wave packets with non-uniform excitation matrix elements, e.g., near a Cooper minimum, have nonhydrogenic dynamics. Photoionization by a delayed probe pulse monitors the wave function near the core, while stimulated emission to the initial state by the probe pulse is sensitive to the fraction of the wave function at a large distance from the core.

[1] J. Parker and C. R. Stroud, Jr., Phys. Rev. Lett. **56**, 716 (1986).

[2] G. Alber, H. Ritsch, and P. Zoller, Phys. Rev. A **34**, 1058 (1986).

[3] J. A. Yeazell and C. R. Stroud, Jr., Phys. Rev. Lett. **60**, 1494 (1988).

[4] L. D. Noordam, A. ten Wolde, and H. B. van Linden van den Heuvell, in *Laser Interactions with Atoms, Solids, and Plasmas*, edited by R. M. More (Plenum Press, New York, 1994).

[5] R. R. Jones and L. D. Noordam, Adv. At., Mol., Opt. Phys. **38**, 1 (1997).

[6] J. H. Hoogenraad and L. D. Noordam, preceding paper, Phys. Rev. A **57**, 4533 (1998), paper I.

[7] A. ten Wolde, L. D. Noordam, A. Lagendijk, and H. B. van Linden van den Heuvell, Phys. Rev. Lett. **61**, 2099 (1988).

[8] J. A. Yeazell, M. Mallalieu, and C. R. Stroud, Phys. Rev. Lett. **64**, 2007 (1990).

[9] J. Wals, H. H. Fielding, and H. B. van Linden van den Heuvell, Phys. Scr. **T58**, 62 (1995).

[10] J. H. Hoogenraad, R. B. Vrijen, and L. D. Noordam (unpublished).

[11] J. H. Hoogenraad, R. B. Vrijen, A. F. G. van der Meer, P. W. van Amersfoort, and L. D. Noordam, Phys. Rev. Lett. **75**, 4579 (1995).

[12] D. Oepts, A. F. G. van der Meer, and P. W. van Amersfoort, Infrared Phys. Technol. **36**, 297 (1995).

[13] J. H. Hoogenraad, R. B. Vrijen, and L. D. Noordam, Phys. Rev. A **50**, 4133 (1994).

[14] M. V. Fedorov, M. Tehranchi, and S. M. Fedorov, J. Phys. B **29**, 2907 (1996).

[15] L. D. Noordam, H. Stapelfeldt, D. I. Duncan, and T. F. Gallagher, Phys. Rev. Lett. **68**, 1496 (1992).

[16] J. H. Hoogenraad and L. D. Noordam, in *Super-Intense Laser-Atom Physics*, Vol. 316 of *NATO Advanced Study Institute, Series B: Physics*, edited by B. Piraux, A. L'Huillier, and K. Rzążewski (Plenum, New York, 1993), pp. 269–278.

[17] R. R. Jones, C. S. Raman, D. W. Schumacher, and P. H. Bucksbaum, Phys. Rev. Lett. **71**, 2575 (1993).

[18] D. I. Duncan and R. R. Jones, Phys. Rev. A **53**, 4338 (1996).

[19] R. Blümel and U. Smilansky, Z. Phys. D **6**, 83 (1987).

[20] R. Blümel, A. Buchleitner, R. Graham, L. Sirko, U. Smilansky, and H. Walther, Phys. Rev. A **44**, 4521 (1991).

[21] O. Benson, A. Buchleitner, G. Raithel, M. Arndt, R. N. Mantegna, and H. Walther, Phys. Rev. A **51**, 4862 (1995).

[22] L. D. Noordam, D. I. Duncan, and T. F. Gallagher, Phys. Rev. A **45**, 4734 (1992).

[23] J. F. Christian, B. Broers, J. H. Hoogenraad, W. J. van der Zande, and L. D. Noordam, Opt. Commun. **103**, 79 (1993).

[24] D. W. Schumacher, J. H. Hoogenraad, D. Pinkos, and P. H. Bucksbaum, Phys. Rev. A **52**, 4719 (1995).

[25] M. Nauenberg, J. Phys. B **23**, L385 (1990).